Catalysis Today 137 (2008) 23–28

Contents lists available at ScienceDirect

Catalysis Today

journal homepage: www.elsevier.com/locate/cattod

Combinatorial approach to the preparation and characterization of catalysts for biomass steam reforming into syngas

Polina Yaseneva [a], Svetlana Pavlova [a,*], Vladislav Sadykov [a], Galina Alikina [a],
Anton Lykashevich [a], Vladimir Rogov [a], Sergey Belochapkine [b], Julian Ross [c]

[a] Boreskov Institute of Catalysis, 5, Pr. Lavrentieva, 630090 Novosibirsk, Russia
[b] Materials & Surface Science Institute, University of Limerick, Limerick, Ireland
[c] Centre of Environmental Research, University of Limerick, Limerick, Ireland

ARTICLE INFO

Article history:
Available online 15 May 2008

Keywords:
Combinatorial synthesis
Bio-oil
Steam reforming of ethanol
Syngas
Ce-Zr mixed oxides
Ru
Pt
Cu-Ni

ABSTRACT

A number of catalysts based on Al_2O_3 loaded with doped Ce-Zr mixed oxides and different active components (Cu, Cu-Ni, Ru, Pt, etc.) were synthesized via standard wet impregnation method using the robotic workstation. Ethanol (EtOH) was taken as a model compound of bio-oil and steam reforming of ethanol (ESR)—as a model reaction. Activity screening experiments performed at 600–700 °C in 0.5 vol.% C_2H_5OH + 2.5 vol.% H_2O + 97 vol.% He mixture revealed that the most effective catalyst composition is $Ru/Ce_{0.4}Zr_{0.4}Sm_{0.2}/Al_2O_3$. Catalytic activity investigations at high reagent concentrations (10 vol.% C_2H_5OH + 40 vol.% H_2O + 50 vol.% N_2) at 650–800 °C confirmed this fact, revealing also that at high temperatures the activity of Cu-Ni catalysts is comparable with that of Ru-containing catalyst.

1. Introduction

In the last years, biomass has been recognized as one of the major world renewable energy sources. Catalytic steam reforming of bio-oil derived from the fast pyrolysis of biomass provides an attractive opportunity to convert it into the hydrogen or syngas from which liquid fuels (gasoline, diesel) and valuable chemicals can be synthesized [1,2]. Bio-oil is a complex mixture of oxygenates (carboxylic acids, aldehydes, ketones, alcohols and phenols), hence, design of an efficient catalyst requires the use of model oxygenate components to establish the composition–structure activity correlations. In this study, we have taken ethanol as a model compound, since it is one of the major components of bio-oil [3–6].

The main problem in steam reforming of bio-oil (and ethanol in particular) is heavy coking of the catalyst leading to its deactivation at temperatures around 470 °C [4,7,8]. To minimize coking and catalyst deactivation, coke precursor gasification and steam activation over the catalyst are to be facilitated [9,10]. Hence, promising systems for design of catalysts for steam reforming of bio-oil appear to be oxides with a high lattice oxygen mobility promoted by metals [4,6,11]. Ceria-zirconia fluorite-like mixed oxides were shown to be quite efficient in preventing coke formation and its removal due to high oxygen storage-release capacity provided by Ce cations [11–13] and an efficient steam activation over Zr cations [5]. Incorporation of low-valence cations (such as La, Gd, Pr) into the lattice of ceria-zirconia solutions is expected to stabilize the lattice and improve the lattice oxygen mobility [14–16]. A wide range of supported active metals (Ni [3,8,10,17,18], Pt, Pd, Rh, Ru [4–6,13,19]) was used for the bio-oil steam reforming processes. To prevent sintering of both mixed oxides and metals at high temperatures, supports with high surface area (Al_2O_3, SiO_2) were used [4,13,19].

Since up for today no stable catalyst for ESR has been developed, the exploring of many compositionally diverse materials could be an efficient solution in finding the active and stable catalyst. Combinatorial approach, which is characterized by the use of robotics and advanced software, was already successfully applied in different fields of heterogeneous catalysis [20]. In this work, the results on the combinatorial synthesis and activity screening of the novel supported catalysts based on doped CeO_2-ZrO_2/Al_2O_3 with

---

* Corresponding author.
E-mail address: pavlova@catalysis.ru (S. Pavlova).

0920-5861/$ – see front matter © 2008 Elsevier B.V. All rights reserved.
doi:10.1016/j.cattod.2008.03.016

different active metals for steam reforming of ethanol into syngas as a model compound of biomass are presented.

2. Experimental

2.1. Catalysts preparation

The catalysts of the general formula $M/Ce_xZr_xY_{1-2x}/\gamma\text{-}Al_2O_3$ designated as $MCZY_{1-2x}$ (M = 7 wt.%. Cu, 1.4 wt.% Pt or Ru, 10 wt.% Cu-Ni or Cu-Ni-Cr; Y = La (L), Pr (P), Sm (S); x = 0.5–0.35; 10 wt.% of $CeZrY_{1-2x}$ mixed oxide) were synthesized by the standard wet impregnation method with two successive impregnation procedures using robotic workstation based on the Hamilton Microlab Duo system [21]. As a support, $\gamma\text{-}Al_2O_3$ (CONDEA Puralox SBa-150, 150 m^2/g) stabilized by 5 wt.% of La was used. After each impregnation, the catalysts were dried overnight in air at 85 °C and then calcined at 800 °C.

2.2. Catalysts characterization

The specific surface area (BET area) was determined by the express BET method using Ar thermodesorption data obtained on a SORBI-M instrument.

The XRD patterns were recorded using a URD-6M diffractometer with Cu Kα radiation in the range of 2θ angles 10–90°.

H_2 TPR experiments were carried out using feed containing 10 vol.% H_2 in Ar at the feed flow rate of 40 ml min^{-1} and temperature ramp 10 °C min^{-1} from ~25 to 900 °C. During the experiment, H_2O was frozen out at −80 °C. The hydrogen concentration was determined using a thermal conductivity detector.

2.3. Catalyst testing

2.3.1. Screening experiments

Catalytic activity in the ESR reaction (standard feed 0.5 vol.% C_2H_5OH + 2.5 vol.% H_2O in He) at short contact times (36–72 ms) was estimated in a flow installation by using a flow quartz reactor (i.d. 2.5 mm) packed with a catalyst (0.25–0.5 mm fraction) diluted with a quartz sand. The screening was performed at 600–700 °C. The products (H_2, CO and CO_2) were continuously monitored by using on-line IR absorbance gas analyzer PEM-2M, TCD and an electrochemical H_2 sensor with the data acquisition and processing through a PC. In these tests, catalysts were heated to the temperature of experiment in the flow of 1 vol.% O_2 in He, and then the reaction mixture was fed till the stationary concentrations of the products were attained.

2.3.2. Catalyst tests at high reagent concentrations

Catalytic experiments in ethanol steam reforming were carried out in U-shaped tubular quartz flow reactor (4.5 mm i.d.) at atmospheric pressure. Usually 0.18 g of pelletized catalyst (fraction 0.5–0.25 mm) diluted in a 1:10 weight ratio with quartz sand was taken. Reaction was performed at 650–800 °C using feed with volume composition $EtOH:H_2O:N_2$ = 1:4:5 fed into the reactor with the total flow rate 9 l/h. Before testing the catalysts were pretreated for 1 h at 400 °C in the flow of 10% H_2 in N_2. Three on-line gas chromatographs (GC) "LHM-8" equipped with thermal conductivity detectors and a flame ionization detector, respectively, were used for the analysis of reactants and products. Hydrocarbons (CH_4, C_2H_6, C_2H_4, etc.) and oxygenates (EtOH, CH_3OH, acetone, diethyl ether, etc.) were analyzed using a Porapak T column; N_2, O_2, CH_4 and CO were analyzed with a molecular sieve column, and H_2, N_2, CO, CO_2, CH_4—with an active carbon "SYT" column. Ar and He were used as carrier gases.

3. Results and discussion

3.1. Catalysts characterization

3.1.1. Surface area and structure

The BET surface area of the initial Al_2O_3 was equal to ~150 m^2/g. The deposition of Ce-Zr-based mixed oxides and active metals caused a moderate decrease of the surface area to 100–120 m^2/g depending on the sample composition.

According to the XRD data, there is no pronounced influence of the dopants nature (La, Sm, Pr) on the alumina support or doped ceria- zirconia oxide structure. Fig. 1 presents the XRD patterns of catalysts with Sm dopant. It could be seen that for all catalysts the main phases are fluorite-like cubic mixed CeO_2-ZrO_2 solid solution (JCPDS 43-1002) and mixed δ- and $\gamma\text{-}Al_2O_3$. For $RuCZS_{0.2}$, the reflections of RuO_2 phase (JCPDS 71-2273) are observed, while for the $PtCZS_{0.2}$ no Pt-containing phases are seen probably due to a high Pt dispersion. In catalysts containing only Cu, CuO (JCPDS 44-0706) phase is observed, whereas for the Cu-Ni-containing sample the intensity of corresponding reflections significantly decreases, while NiO phase is not detected. The latter along with the shift of reflections corresponding to Al_2O_3 in Cu-Ni sample (Fig. 1) could be due to a partial Ni^{2+} incorporation into alumina and formation of a highly dispersed surface spinel of Ni and Cu [22].

3.1.2. Temperature-programmed reduction

H_2-TPR method was used to investigate redox properties of catalysts and oxygen mobility. As an example, H_2-TPR spectra of Cu catalysts doped by La, Cu-Ni-(Cr) doped by Sm and Ru catalysts doped by Sm are presented in Figs. 2–4, respectively, illustrating the effect of dopant content on the catalyst reduction features.

For the Cu-containing catalysts, the main reduction takes place below 400 °C (Fig. 2). In the TPR spectra, the low-temperature peak could be mainly assigned to the reduction of different copper forms (highly dispersed surface/bulk copper oxidic species) [23], though reduction of some Ce^{4+} cations could not be excluded as well [24]. Due to rather low (10 wt.%) content of doped ceria-zirconia solid solution in samples, its reduction degree at low temperatures could not be estimated with any reasonable precision. A high-temperature reduction tail (Fig. 2) can be mainly assigned to reduction of ceria-zirconia solid solution. The position of low-temperature (~240 °C) maximum slightly shifts upward with La content, perhaps reflecting some stabilization of Cu^{2+} cations by

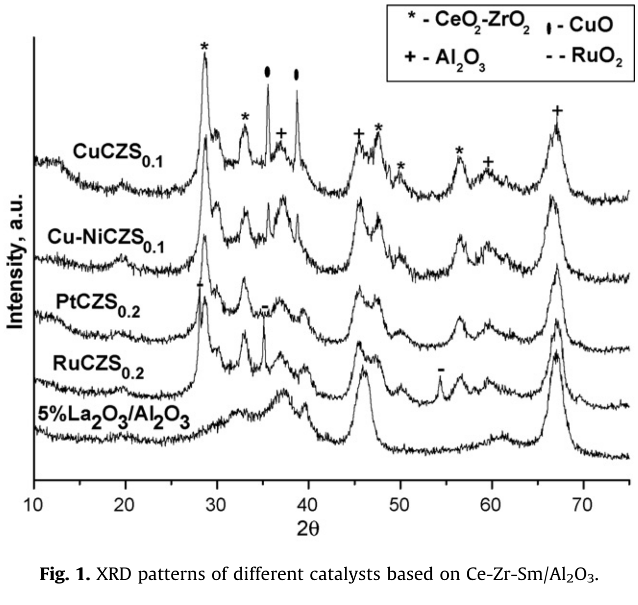

Fig. 1. XRD patterns of different catalysts based on Ce-Zr-Sm/Al_2O_3.

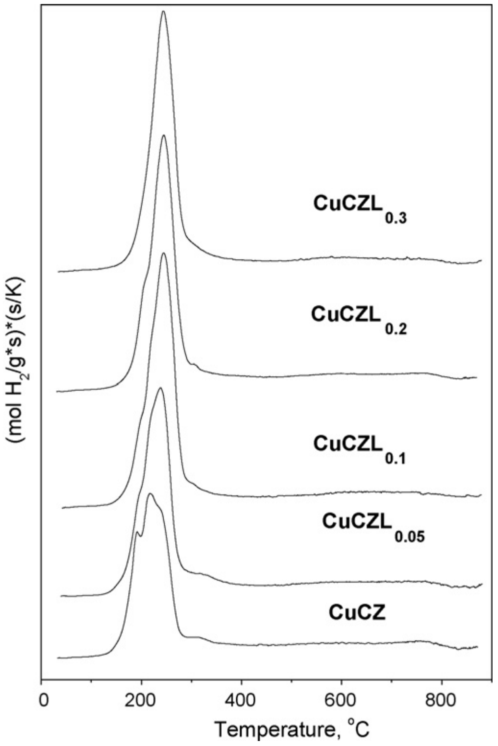

Fig. 2. H_2 TPR spectra of $CuCZL_{1-2x}$ catalysts.

basic La cations with formation of some perovskite-like fragments. Similarly, the total amount of H_2 consumed in the low-temperature peak depends on the La concentration reaching a maximum for $CuCZL_{0.1}$ sample (Table 1), thus suggesting the highest surface oxygen mobility for this composition. Since H_2/Cu ratio calculated from these data is <1 (~0.7), this implies that a part of Cu cations incorporated into the bulk of samples is not reduced in these low-temperature peaks.

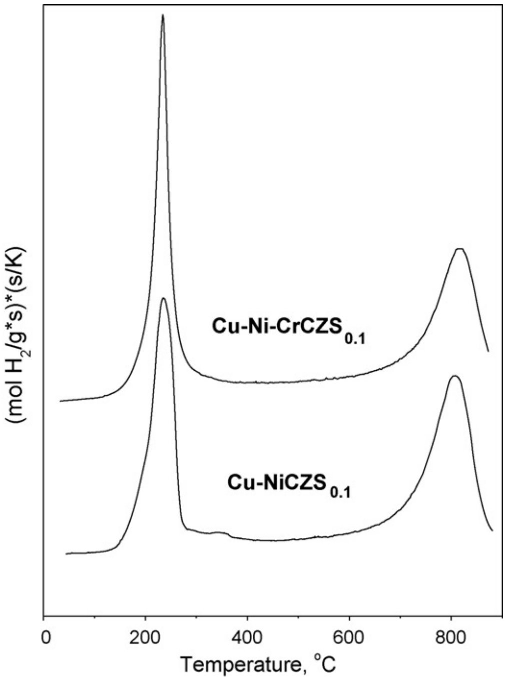

Fig. 3. H_2 TPR spectra of Cu-Ni-(Cr)$CZS_{0.1}$ catalysts.

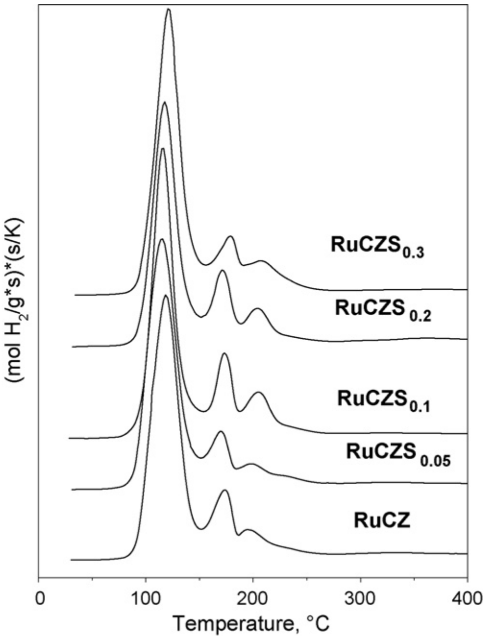

Fig. 4. H_2 TPR spectra of $RuCZS_{1-2x}$ catalysts.

The H_2-TPR spectra of all Cu-Ni- and Cu-Ni-$CrCZY_{1-2x}$ catalysts (Fig. 3) along with a low temperature peak at ~230 °C assigned to reduction of Cu^{2+} cations show a high-temperature peak at 800 °C which is absent in the case of $CuCZY_{1-2x}$ samples. This peak could correspond to the reduction of surface Ni-containing perovskite and/or spinel.

The character of TPR spectra of $RuCZS_{1-2x}$ catalysts (Fig. 4) does not depend on the Sm concentration. For all samples, three reduction peaks are observed: a highly intensive one at 114–120 °C and two others with a lower intensity situated at 170–179 and 197–206 °C, respectively. These maxima could be mainly assigned to the reduction of RuO_2 particles/species with different dispersion [25]. The hydrogen consumption depends on the Sm concentration, with the maximum being attained for the $RuCZS_{0.2}$ composition (Table 1).

These H_2-TPR data suggest that the highest surface/lattice oxygen mobility and reactivity are achieved at a proper additive content. This is why for the first activity screening tests the Cu-containing catalysts with dopant content 0.1 mole fraction and noble metal (Pt, Ru)-containing catalysts with dopant content 0.2 mole fraction were mainly chosen (vide infra).

3.2. Catalysts screening

In the screening experiments, concentrations of H_2 and CO products were chosen as parameters characterizing catalytic activity. Figs. 5 and 6 show the effect of dopant concentration in Ce-Zr oxide on the activity of Cu catalysts doped by La and over Pt and Ru catalysts doped by Sm. It could be seen that for copper-containing catalysts, H_2 concentration goes through the maximum

Table 1
Hydrogen consumption over $CuCZL_{1-2x}$ and $RuCZS_{1-2x}$ catalysts

Catalyst	mmol H_2/g_{Cat} (30–400 °C)	Catalyst	mmol H_2/g_{Cat} (30–400 °C)
CuCZ	0.696	RuCZ	0.270
$CuCZL_{0.05}$	0.743	$RuCZS_{0.05}$	0.260
$CuCZL_{0.1}$	0.823	$RuCZS_{0.1}$	0.264
$CuCZL_{0.2}$	0.816	$RuCZS_{0.2}$	0.284
$CuCZL_{0.3}$	0.793	$RuCZS_{0.3}$	0.271

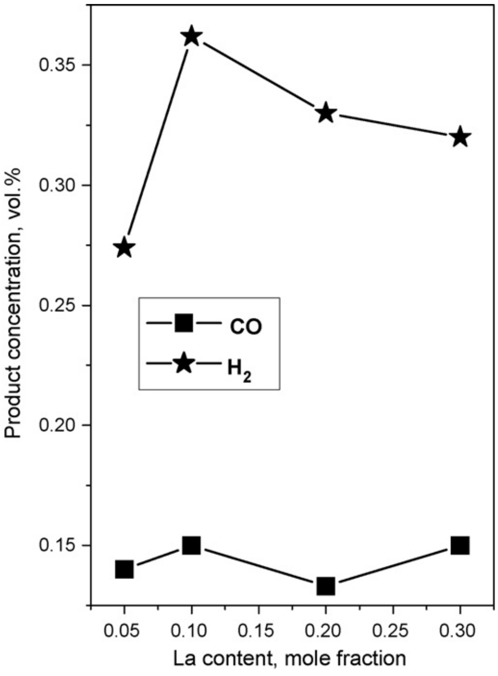

Fig. 5. H_2 and CO concentrations obtained over $CuCZL_{1-2x}$ catalysts at 600 °C in the screening tests, contact time 72 ms.

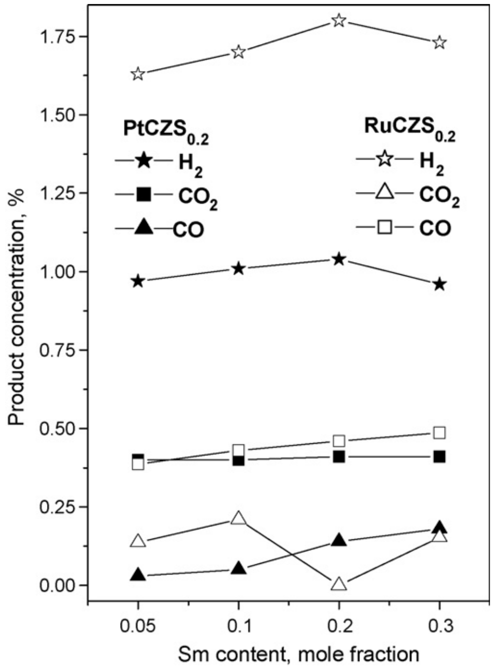

Fig. 6. H_2, CO and CO_2 concentrations obtained over $PtCZS_{1-2x}$ and $RuCZS_{1-2x}$ catalysts at 700 °C in the screening tests, contact time 36 ms.

at La content equal to 0.1 mole fraction ($CuCZL_{0.1}$). This fact is in a good agreement with H_2-TPR data revealing the maximal amount of active oxygen removed in the low-temperature peak at this La concentration. For Pt and Ru-containing catalysts doped with Sm, the most effective samples contain 0.2 mole fraction of the dopant, which also agrees with TPR data and further justifies selection of samples series for screening tests (vide supra).

The ESR activity of catalysts containing the same active metals is certainly affected by the nature of dopant. For instance, the maximum of H_2 and CO concentration is observed for the $CuCZY_{1-2x}$ catalysts with Sm dopant, for Cu-Ni-containing catalysts without dopants and for Cu-Ni-Cr catalysts with Pr dopant (Fig. 7).

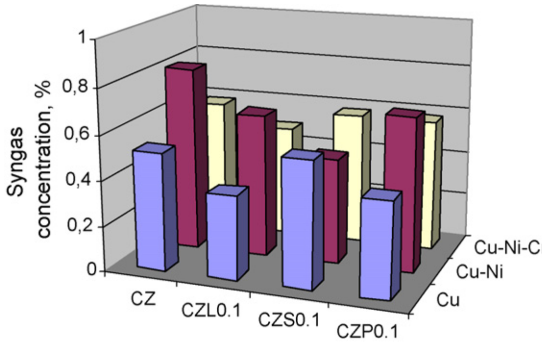

Fig. 7. Syngas (H_2 + CO) concentration obtained over Cu- and Cu-Ni-containing catalysts at 600 °C in the screening tests, contact time 72 ms.

Screening investigation of the dopant nature influence on the catalyst activity over samples containing Pt or Ru has shown that among Ru-containing catalysts the sample doped by Sm is the most effective (Fig. 8). Among Pt-containing catalysts, the sample doped by La is the most active (Fig. 9). At 700 °C, Ru-containing catalysts are more active than those containing Pt. As concerning the active metals, in general, Ru-containing catalysts are the most active. Among Cu-containing catalysts, Cu-NiCZ and Cu-Ni-$CrCZP_{0.1}$ catalysts are the most effective (Fig. 10).

3.3. Catalysts tests at high reagent concentrations

The most effective samples chosen according to the results of screening experiments $RuCZSm_{0.2}$, Cu-NiCZ, $CuCZSm_{0.1}$, Cu-Ni-$CrCZP_{0.1}$, $PtCZSm_{0.2}$ were studied in ESR at high reagent concentrations.

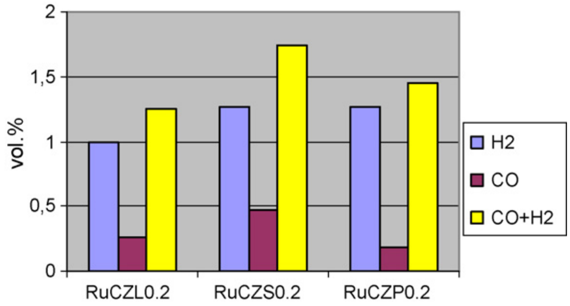

Fig. 8. H_2, CO and syngas concentrations obtained over Ru-containing catalysts at 700 °C in the screening tests, contact time 36 ms.

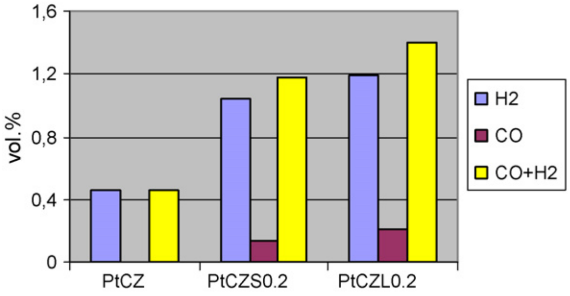

Fig. 9. H_2, CO and syngas concentrations obtained over Pt-containing catalysts at 700 °C in the screening tests, contact time 36 ms.

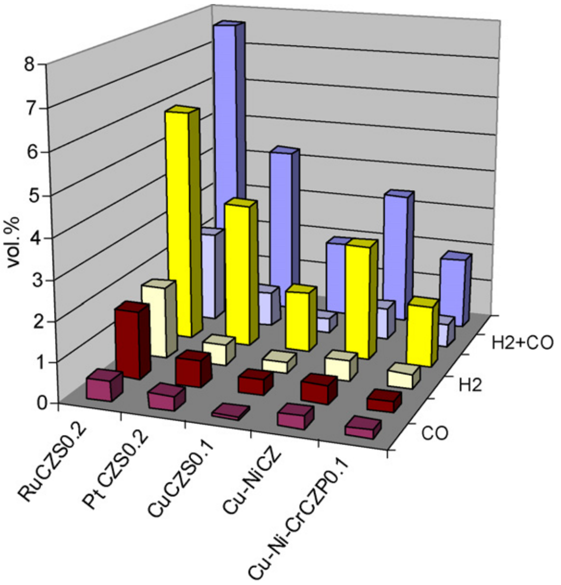

Fig. 10. Comparison of CO, H_2 and syngas concentrations obtained at 600 °C in screening tests (first row) and in activity study at high reagent concentrations (second row) in ESR over the most effective catalysts, contact time 72 ms.

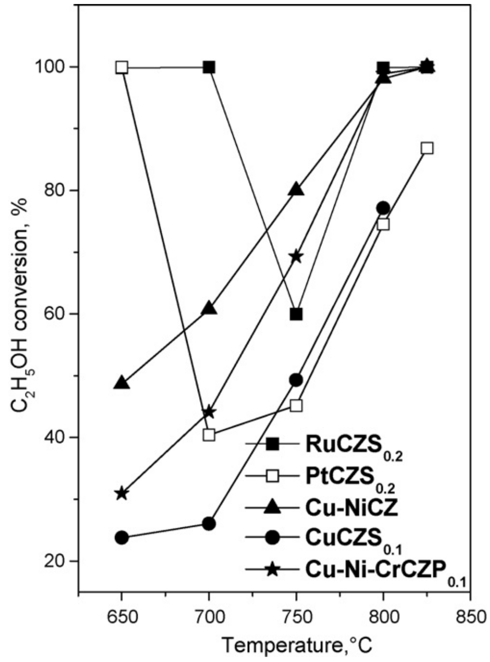

Fig. 11. Ethanol conversion over the most effective catalysts (according to the screening tests) in the activity study at high reagent concentrations, contact time 72 ms.

For Ru or Pt-containing samples EtOH conversion at 650 °C is 100% (Fig. 11) declining at 700–750 °C and then further increasing at higher temperatures. This unusual behavior can be explained with a due regard for variation of the products selectivity with temperature (Fig. 12a). In all the temperature range (650–800 °C), over $RuCZS_{0.2}$ sample (Fig. 12a) as well as for $PtCZS_{0.2}$ catalysts (not shown for brevity), ethylene selectivity declines with temperature while CO and H_2 selectivity increases. This suggests that at lower temperatures mainly dehydration reaction takes place, while at higher temperatures steam reforming reaction predominates. Since dehydration is catalyzed by the acidic sites of the support, a decline of EtOH conversion with temperature can be assigned to the surface coking due to oligomerization of ethylene species. The increase of the surface oxygen mobility with the temperature facilitates coke gasification which accelerates steam reforming reaction. This scheme agrees with the results of earlier studies of ethanol steam reforming on alumina-supported 1% Rh/40% $Ce_{0.8}Zr_{0.2}/Al_2O_3$ [19] or 0.75% Pt/10% CeO_2/Al_2O_3 [26] catalysts. In both cases, at moderate (500–850 K) temperatures ethanol dehydration into ethylene was shown to be the primary process followed by the formation of syngas at higher temperatures. Presence of CH_3OH and CH_4 in the products (Fig. 12) implies occurrence of cracking reactions as well.

For the Cu- and Cu-Ni-containing catalysts, conversion increases in all the temperature range (Fig. 11), suggesting either a lower acidity of the surface sites or participation of surface Cu/Ni species in gasification of coke precursors. The activity of these catalysts decreases in the next order: Cu-NiCZ > Cu-Ni-$CrCZPr_{0.1}$ > $CuCZS_{0.1}$. For Cu-NiCZ sample conversion of ethanol at 750 °C exceeds 80%. The hydrogen concentration and CO

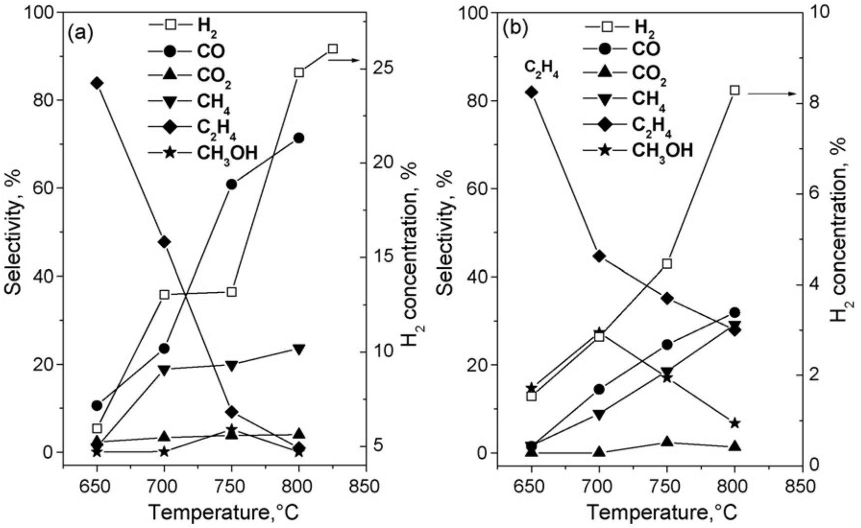

Fig. 12. H_2 concentration and C-products selectivities over the most effective $RuCZS_{0.2}$ (a) and the less effective $CuCZS_{0.2}$ (b) catalysts in the activity study at high reagent concentrations (T = 650–800 °C), contact time 72 ms.

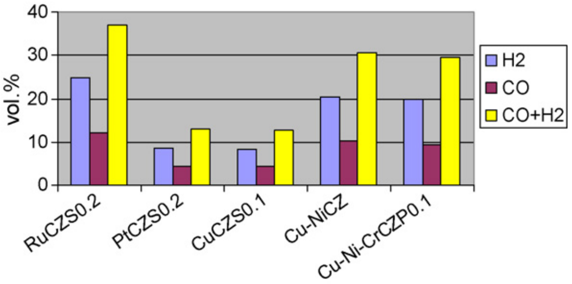

Fig. 13. H_2, CO and syngas concentrations obtained over the most effective catalysts at 800 °C in activity study at high reagent concentrations, contact time 72 ms.

Table 2
C-product balances calculated for the most effective catalysts at high reagent concentrations and 800 °C

Catalyst	Balance (800 °C)
$RuCZS_{0.2}$	102
$PtCZS_{0.2}$	100
$CuCZS_{0.1}$	101
Cu-NiCZ	82
Cu-Ni-$CrCZP_{0.1}$	99

selectivity strongly depend on the temperature. At 650 °C, the highest hydrogen production is observed over the Ru and Pt-containing catalysts, whereas the highest CO selectivity at this temperature is found for Cu-NiCZ catalyst. At 800 °C, $RuCZS_{0.2}$ catalyst again exhibits the highest H_2 yield, the lowest one is observed over $PtCZS_{0.2}$ and $CuCZS_{0.1}$ samples (Fig. 12b). While CO selectivity is ~70% over $RuCZS_{0.2}$, Cu-NiCZ and Cu-Ni-$CrCZP_{0.1}$ catalysts, over the $PtCZS_{0.2}$ and $CuCZS_{0.1}$ samples it attains only ~30%. The low CO selectivities for the latter catalysts could be due to predomination of the dehydration reaction over the steam reforming reactions, which follow from the presence of a considerable amount of ethylene even at 800 °C. Moreover, formation of by-product methane indicates occurrence of cracking reactions.

As far as the yield of desired products (H_2, CO) is concerned, at 600 °C (Fig. 10) the data obtained at high concentrations reasonably agree with results of screening tests: the highest H_2 and syngas concentrations are observed over $RuCZS_{0.2}$ and the lowest ones are found for $CuCZS_{0.1}$ catalyst. This demonstrates usefulness of screening experiments carried out with diluted feeds in the limited temperature range. However, as expected, increasing of reaction temperature results in some variation of the product distribution. Thus, at 800 °C H_2 and syngas production over Cu-NiCZ catalyst is comparable with that for $RuCZS_{0.2}$ catalyst (Fig. 13).

As concerning the catalyst stability to coking, the data on the carbon balance could be a characteristics of a catalyst coking resistance. Thus, for the Cu-NiCZ catalyst, the carbon balance being equal to ~80% (Table 2) shows that though the catalyst provides for a high concentration of synthesis gas, it is subjected to a noticeable coking. Addition of Cr into the catalyst allows to suppress the coke formation and attain the carbon balance value close to 100% (Table 2). The activity of the most effective $RuCZS_{0.2}$ catalyst was practically unchanged during all the time of prolonged experiments at varied contact times (the data will be presented in the next work). In fact, this implies that $RuCZS_{0.2}$ catalyst is not subjected to coking that is confirmed by a well carbon balance close to 100% (Table 2).

4. Conclusions

Using robotic workstation, a number of catalysts based on Al_2O_3 loaded with doped Ce-Zr mixed oxides and different active components (Cu, Cu-Ni, Ru, Pt, etc.) were successfully synthesized. Results on screening tests of ESR catalyst activity reasonably agree with the data obtained at high reagent concentrations and show that the activity of the catalysts in terms of the syngas yield decreases in the row: $RuCZS_{0.2} > PtCZS_{0.2} >$ Cu-NiCZ > Cu-Ni-$CrCZP_{0.1}$. However, the Cu-NiCZ sample is appreciably subjected to coking, whereas all other are sufficiently stable to coking. Some correlations of catalytic performance with the surface/lattice oxygen mobility and reactivity changed due to the dopant nature and content were observed.

Acknowledgement

The authors acknowledge the financial support of INTAS 05-1000005-7663 project.

References

[1] A. Demirbras, Prog. Energy Combust. Sci. 33 (2007) 1.
[2] M. Asadullah, S. Ito, K. Kunimori, M. Yamada, K. Tomishige, J. Catal. 208 (2002) 255.
[3] X. Hu, G. Lu, J. Mol. Catal. A 261 (2006) 43.
[4] C. Rioche, S. Kulkarni, F.C. Meunier, J.P. Breen, R. Burch, Appl. Catal. B 61 (2005) 130.
[5] K. Takanabe, K. Aika, K. Seshan, L. Lefferts, Chem. Eng. J. 120 (2006) 133.
[6] E.E. Iojoiu, M.E. Domine, T. Davidian, N. Guilhaume, C. Mirodatos, Appl. Catal. A 323 (2007) 147.
[7] D.L. Trimm, Catal. Today 37 (1997) 233.
[8] A.N. Fatsikostas, X.E. Verykios, J. Catal. 225 (2004) 439.
[9] K. Takanabe, K. Aika, K. Seshan, L. Lefferts, J. Catal. 227 (2004) 101.
[10] L. Garcia, R. French, S. Czernik, E. Chornet, Appl. Catal. A 201 (2000) 225.
[11] V.A. Sadykov, T.G. Kuznetsova, G.M. Alikina, Yu.V. Frolova, A.I. Lukashevich, V.S. Muzykantov, V.A. Rogov, L.Ch. Batuev, V.V. Kriventsov, D.I. Kochubei, E.M. Moroz, D.A. Zyuzin, E.A. Paukshtis, E.B. Burgina, S.N. Trukhan, V.P. Ivanov, L.G. Pinaeva, Yu.A. Ivanova, V.G. Kostrovskii, S. Neophytides, E. Kemnitz, K. Scheurel, C. Mirodatos, in: K. David, McReynolds (Eds.), New Topics in Catalysis Research, Nova Publishers, NY, 2006, pp. 97–196.
[12] H. He, H.X. Dai, C.T. Au, Catal. Today 90 (2004) 245.
[13] K. Tomishige, M. Asadullah, K. Kunimori, Catal. Today 89 (2004) 389.
[14] J. Kašpar, P. Fornasiero, Catalysis by ceria and related materials, in: A. Trovarelli (Ed.), Catalytic Science Series, vol. 2, Imperial College Press, London, UK, 2002, p. 217.
[15] P. Vidmar, P. Fornasiero, J. Kašpar, G. Gubitosa, M. Graziani, J. Catal. 171 (1997) 160.
[16] G.L. Markaryan, L.N. Ikryannikova, G.P. Muravieva, A.O. Turakulova, B.G. Kostyuk, E.V. Lunina, V.V. Lunin, E. Zhilinskaya, A. Aboukais, Colloids Surf. A 151 (1999) 435.
[17] T. Wang, J. Chang, X. Cui, Q. Zhang, Y. Fu, Fuel Process. Technol. 87 (2006) 421.
[18] D. Srinivas, C.V.V. Satyanarayana, H.S. Potdar, P. Ratnasamy, Appl. Catal. A 246 (2003) 323.
[19] T. Montini, L.D. Rogatis, V. Gombac, P. Fornasiero, M. Graziani, Appl. Catal. B 71 (2007) 125.
[20] A. Hagemeyer, B. Jandeleit, Y. Liu, D.M. Poojary, H.W. Turner, A.F. Volpe, W.H. Weinberg, Appl. Catal. A 221 (2001) 23.
[21] G. Grasso, B. Harji, E. Xue, S. Belochapkine, J.R.H. Ross, Catal. Today 81 (2003) 369.
[22] C.O. Arean, J.S. Vinuela, J. Solid State Chem. 60 (1985) 1.
[23] W.-P. Dow, Y.-P. Wang, T.-J. Huang, Appl. Catal. A 190 (2000) 25.
[24] X. Tang, B. Zhang, Y. Li, Y. Xu, Q. Xin, W. Shen, Appl. Catal. A 288 (2005) 116.
[25] B. Faroldi, C. Carrara, E.A. Lombardo, L.M. Cornaglia, Appl. Catal. A 319 (2007) 38.
[26] R.M. Navarro, M.C. Álvarez-Galván, M. Cruz Sánchez-Sánchez, F. Rosa, J.L.G. Fierro, Appl. Catal. B 55 (2005) 229.